Design and Testing of a New Cooling System using Solid Nitrogen for Pulsed Field Magnetization and Characterization of HTS Bulks

Ghazi Hajiri, Kévin Berger, Jean Lévêque

Design and Testing of a New Cooling System using Solid Nitrogen for Pulsed Field Magnetization and Characterization of HTS Bulks

G Hajiri[1,*], K Berger[1] and J Lévêque[1]

[1]Université de Lorraine, GREEN, F-54000 Nancy, France

*ghazi.hajiri@univ-lorraine.fr

Abstract. Solid Nitrogen (SN_2) can provide a uniform and stable cryogenic environment for High Temperature Superconducting (HTS) systems such as bulk samples during their magnetization and/or characterization. In this paper, a SN_2 cooling system consisting of a cryocooler Sumitomo CH-110 and an exchanger in a Liquid Nitrogen (LN_2) bath is studied. In order to design this cooling system, an analytical model based on a nodal method coupled to a formulation of the thermal capacity was realized. The model considers the thermal parameters variation as well as the phase change of the Nitrogen. In order to compare our results, we performed a 3D simulation on COMSOL Multiphysics. The performance of the cooling system was evaluated by measurements and we estimate that 10 L of LN_2 can be cooled down to 25 K in 45 hours.

1. Introduction

As shown in [1], thermal effects are the greatest limitation for controlling the magnetization of superconducting bulks during a Pulsed Field Magnetization (PFM) method. The performances of High Temperature Superconductors (HTS) are enhanced by decreasing their operating temperature [2]. Thus, we aim to obtain a more comfortable environment by freezing and cooling a Liquid Nitrogen (LN_2) bath down to 25 K. In addition, a cold mass can be a reliable solution in superconducting applications [3–7]. Several methods have been developed to study the phase changes of materials. The present enhanced enthalpy method has been considered a theoretical basis for the description and prediction of complex cooling and thermal processes [8]. Some others have proposed a stepwise thermal analysis of a cooling, i.e. thermal capacities are defined for each phase: liquid, solid, and solid under 35.6 K [9].

In this paper, a whole cryogenic system for freezing LN_2 is studied. It consists of a cryostat, manufactured by Cryo Diffusion, a Sumitomo CH-110 cryocooler and a homemade Oxygen-Free High Thermal Conductivity (OFHC) heat exchanger as shown in figure 1. We simulate the cooling and freezing process from an analytical nodal method coupled with a Heat Capacity Formulation (HCF-Nodal-Model). We also compared our model with a numerical simulation based on a 3D Finite Element Method (FEM) implemented on COMSOL Multiphysics software.

2. Cooling system

The heat transfer from the cold head to the LN_2 bath is achieved by thermal conduction thanks to a proper heat exchanger. The heat exchanger figure 1 consists of a 5 mm thick square plate of 440 mm side length. The choice of this shape was made in order to homogenize the temperature in the radial

direction since the cold head is not located at the center of the system. Four rods are then placed on the bottom of the LN_2 bath and connected to the thick square plate using flexible thermal links, the rods are 540 mm long and have a square cross-section of 30x30 mm², each bar is connected with two flexible bars to ensure a good continuity of heat flow, as an example the bar number 10 is connected to the square plate with two flexible bars 6^a and 6^b. The four rods 10, 11, 12 and 13 are brazed using silver on the heat exchanger 14, which is made from a copper plate of 1 mm thick, 150 mm wide and 2 m of perimeter rolled on a 250 mm diameter. This heat exchanger was manufactured in our laboratory and corrugated in order to increase the heat exchange surface. The whole set of copper parts weighs about 40 kg.

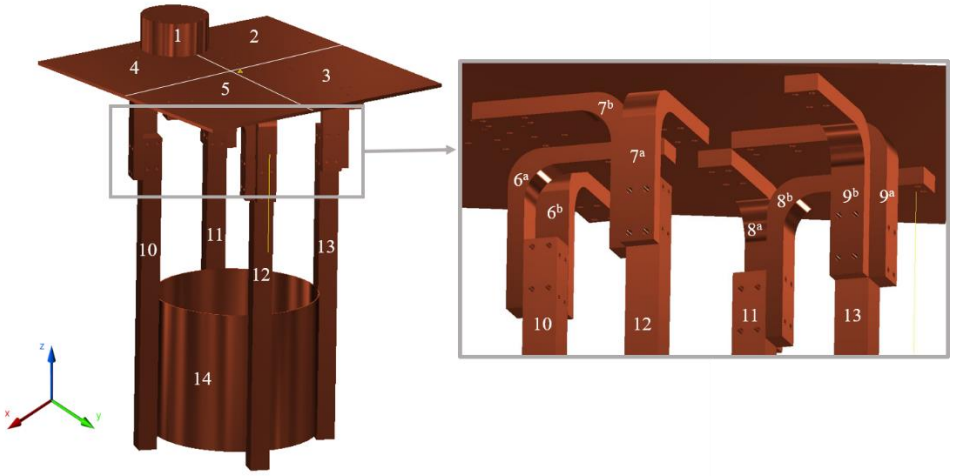

Figure 1. 3D view of the heat exchanger fabricated in our laboratory designed to solidify nitrogen using a Sumitomo CH-110 cryocooler and the notation of the different parts implemented in our nodal model.

3. Analytical model

The design and sizing of the cooling system requires an analysis of the geometry and the choice of materials for the different components of the system. This analysis requires a fast and effective model for the sizing process. The 3D finite element calculation is easy to implement and likely to be precise but requires an important computation time. Therefore, an analytical model is detailed in this section to provide a more efficient design tool. The analytical model is a thermal nodal network, the initial network comprised only few nodes and was further expanded to account for the complex parts of the heat exchanger and the LN_2 bath until reaching the following model.

3.1. Nodal analysis

The temperature variation of each element is calculated using a nodal method. A network of thermal resistors and capacitors has been developed according to the geometry of our system and used to solve the heat diffusion equation [10]:

$$\rho C_p \frac{dT}{dt} = P_v + \mathrm{div}\left(k \cdot \overrightarrow{\mathrm{grad}}\, T\right) \quad (1)$$

where ρ is the density, C_p the heat capacity, P_v the power per unit of volume and k the thermal conductivity. In fact, the cooling system is divided into several equivalent thermal elevations. As shown in figure 2a, each component of the cooling system is represented by a uniform thermal capacity and a thermal resistance network, The formulas for the thermal resistance in the different directions are presented in Table 1 in [11]. For our cooling case, the cryocooler head is in contact with the upper boundary of the part number 1 as shown in figure 1. For this purpose, we define a cooling power

generator on the boundary of the part number 1. Furthermore, the nitrogen bath was discretized in the radial direction to study the thermal gradient. As shown in figure 2b for the temperature analysis, we apply the analogy with Kirchhoff's law [12] and realize a flux analysis on all the nodes so that:

$$C_{\mathrm{n}} \frac{dT_{\mathrm{n}}}{dt} = P_{\mathrm{n}} + \sum_{m=1}^{i} G_{\mathrm{nm}} (T_{\mathrm{m}} - T_{\mathrm{n}}) \tag{2}$$

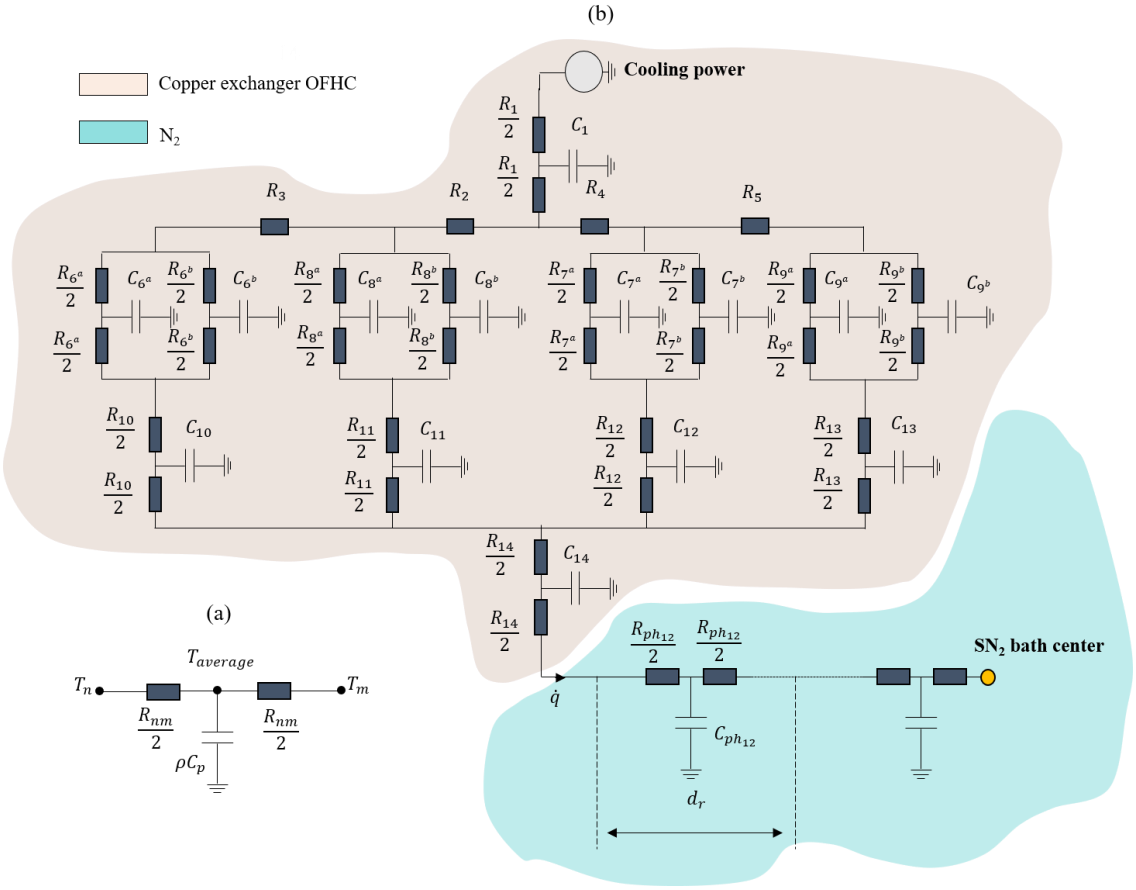

Figure 2. (a) Thermoelectric circuit by analogy of a single element, (b) Simplified schematic of the nodal network, the beige area represents the copper parts and the blue area represents the radial discretization in the nitrogen bath. The indexes of each resistance and thermal capacity of the copper part correspond to the numbering of the parts indicated in figure 1.

where *n* is the node under study, *i* is the set of nodes and *P* is the heat source injected at a node *n*. G_{nm} is the thermal conductance, it is equal to the inverse of the thermal resistance R_{nm}, ie $G_{\mathrm{nn}} = 1/R_{\mathrm{nm}}$. The equations are then written in a matrix form:

$$[C] \times \dot{T} = [A] \times T + P \tag{3}$$

with $A_{\mathrm{nm}} = G_{\mathrm{nm}}$ and $A_{\mathrm{nn}} = -\sum_{m=1}^{i} G_{\mathrm{nm}}$. As shown in [13], the heat capacity matrix [*C*] is a diagonal matrix, [*A*] is the thermal conductance matrix and *P* is the cooling power vector. The thermal conductances A_{nn} and A_{nm} represent the diagonal and non-diagonal terms of the conductance matrix A, respectively.

3.2. Phase change

In this study, the thermal properties of the nitrogen C_p and k, and the cryocooler power are functions of the temperature. However, a constant density ρ is defined for both liquid and solid phase.

To account for phase change, the thermal equation is solved after specifying the properties of a phase change material based on the apparent heat capacity formulation [8]. The principle here is to add the latent heat L to the energy balance equation exactly when the material reaches its phase change temperature T_{pc}. It is assumed that the transformation takes place in a temperature range ΔT around T_{pc} as shown in figure 3. In this interval, the phase of the material is modelled by a smoothed function, θ, representing the phase fraction before the transition, which is equal to 1 before $T_{pc} - \Delta T/2$ and 0 after $T_{pc} + \Delta T/2$. The specific enthalpy H is expressed by:

$$H = \theta(T) H_{ph1} + (1-\theta(T)) H_{ph2} \tag{4}$$

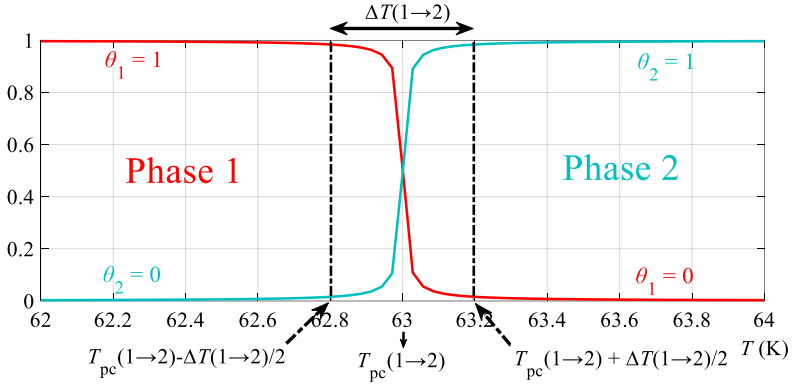

Figure 3. Smoothed transition functions θ_1 and θ_2 between phase 1 and phase 2.

wherein the indexes "ph1" and "ph2" indicate the phases, respectively solid and liquid. By differentiating with respect to temperature, the equality (4) gives the following formula for the specific heat capacity:

$$C_p(T) = \left(\theta_1(T) C_{p,ph1}(T) + \theta_2(T) C_{p,ph2}(T)\right) + \left(H_{ph2} - H_{ph1}\right) \frac{d\beta_m(T)}{dT} \tag{5}$$

where β_m is the mass fraction here equal to:

$$\beta_m(T) = \frac{1}{2}\left(\theta_2(T) - \theta_1(T)\right) \tag{6}$$

since a constant density ρ is assumed in both phases. In the perfect case, when θ_1 is the Heaviside functions, i.e. equal to 1 before T_{pc} and 0 after T_{pc}, and conversely for θ_2, $d\beta_m / dT$ is a Dirac pulse. Finally, the effective thermal conductivity reduces to:

$$k(T) = \theta_1(T) k_{ph1}(T) + \theta_2(T) k_{ph2}(T) \tag{7}$$

4. Experimentation process

As shown in figure 4a, Sumitomo's CH110 77K cryocooler was used as the cooling source powered by an F70-cooled compressor to provide helium circulation. In addition, a conventional Pfeiffer Hi-Cube 300 vacuum pump was used for pumping. Figure 4b shows the main steps used for the solidification of nitrogen, the first step is to start the precooling of the cold head and the cooling system to 77 K, then the cryocooler is stopped and the bath is filled with liquid nitrogen. For this purpose, temperature sensors have been placed at different levels of the bath to determine the level of nitrogen filling. Then, the

cooling with the cryocooler is restarted and the pumping begin to ensure a good vacuum inside the cryostat.

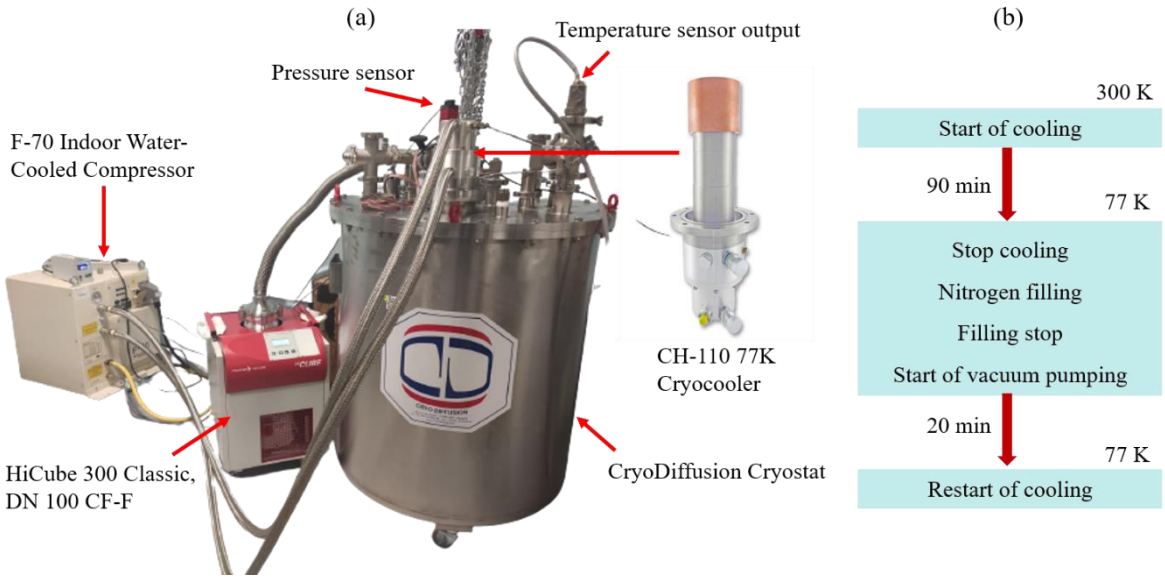

Figure 4. (a) Overview of all the cooling system, (b) Process applied in order to solidify nitrogen.

5. Results

5.1. Test of the heat exchanger without load (without liquid nitrogen)

Various tests were performed to ensure the correct design of the cooling system. First, the cooling system was tested under no load, i.e. without liquid nitrogen. Figure 5a shows the temperature distribution of the different elements of the exchanger. The index of each temperature corresponds to the sensor location according to figure 1. It can be noticed that to cool about 40 kg of OFHC copper using a Sumitomo CH110 77 K cryocooler, it requires 8 h of cooling at an initial temperature of 298 K. In addition, the average cooling rate was 34 K/h. Figure 5b shows the temperature of the different elements in steady state at t = 10 h. The temperature difference between the hottest point T_{14} and the

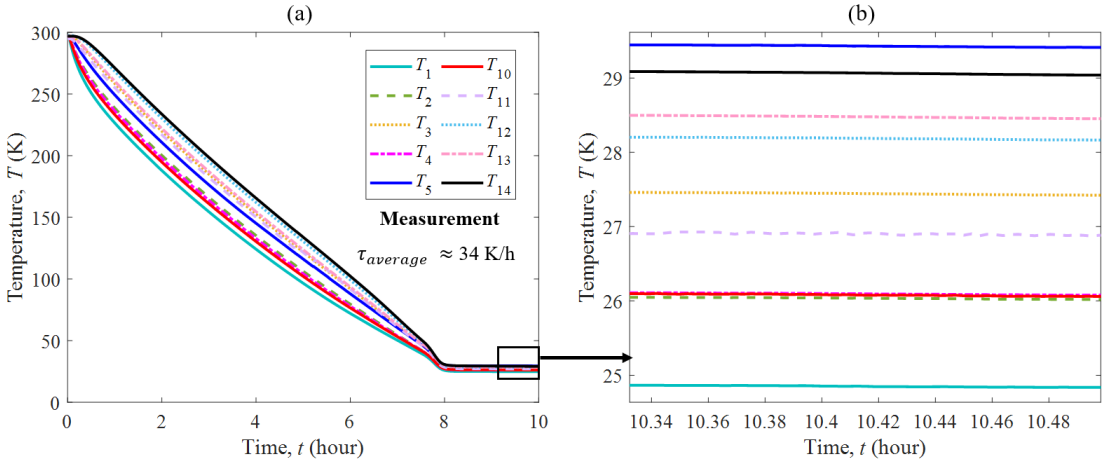

Figure 5. (a) A no-load test of the temperature of the different cooling system elements as a function of time, (b) Steady state temperature in the interval of 10 hours after the start of cooling. The indices of each sensor correspond to the part numbering shown in figure 1.

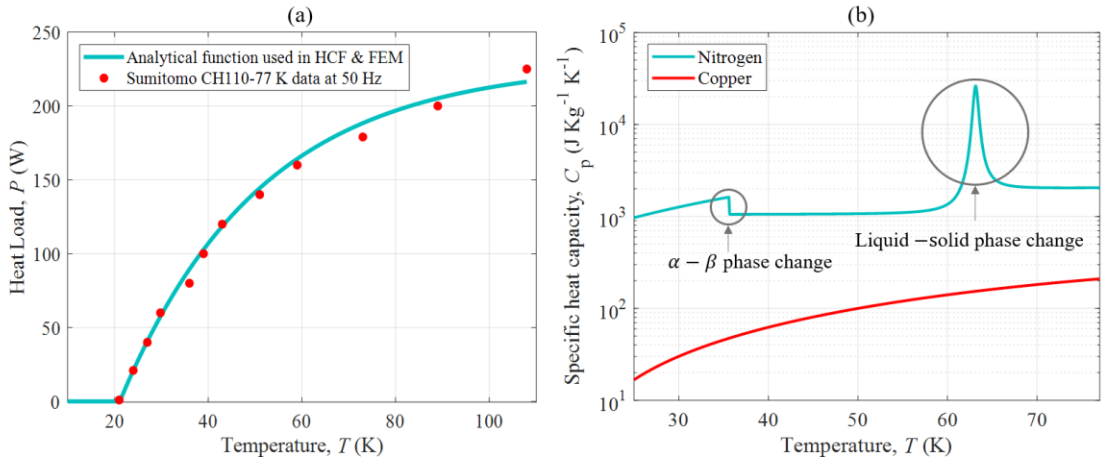

Figure 6. (a) Analytical formula of the cooling capacity of the Sumitomo cryocooler CH-110 77K, (b) Analytical expression of the variation of the specific heat of copper and nitrogen used in HCF-Nodal-Model and FEM.

coldest point T_1 in steady state was about 4.5 K. In other words, T_1 = 24.9 K and T_{14} = 29.4 K. In addition, the location of the hottest and coldest points allows us to place only two sensors instead of ten on the exchanger in order to see the behavior of the exchanger during nitrogen solidification tests.

5.2. Load testing and validation of model performance

In this section, an evaluation of the performances of the previously presented model through a comparison with a 3D FEM calculation and measurements is performed. The HCF analytical model is based on the coupling of a nodal method and a heat capacity formulation, the thermal conductivity is considered constant and equal to 0.15 W/m/K [14,15] and 0.33 W/m/K [16] during the liquid and the solid phase respectively. The study of the problem is transient and ensured by the "ode15s" solver in Matlab software, the relative tolerance is equal to 10^{-3} and a maximum step time of 10^{-2} s has been used. The 3D FEM model is realized on COMSOL-Multiphysics software. The physic module used in this software is heat transfer in fluids. The model of the nitrogen is defined as a fluid with a liquid-solid phase change at 63.1 K. The thermal conductivities of materials are defined as varying with temperature [17,18]. The latent heat L of the liquid-solid phase change is defined in the same way in both models, it is equal to approximately 25 kJ/kg [19]. As shown in figure 6a, an analytical function is defined as the cooling power of the CH-110 77K cryocooler [20]. Based on the data [21] and [22], figure 6b shows the analytical expression of the variation of the specific heat of copper and nitrogen used in HCF-Nodal-

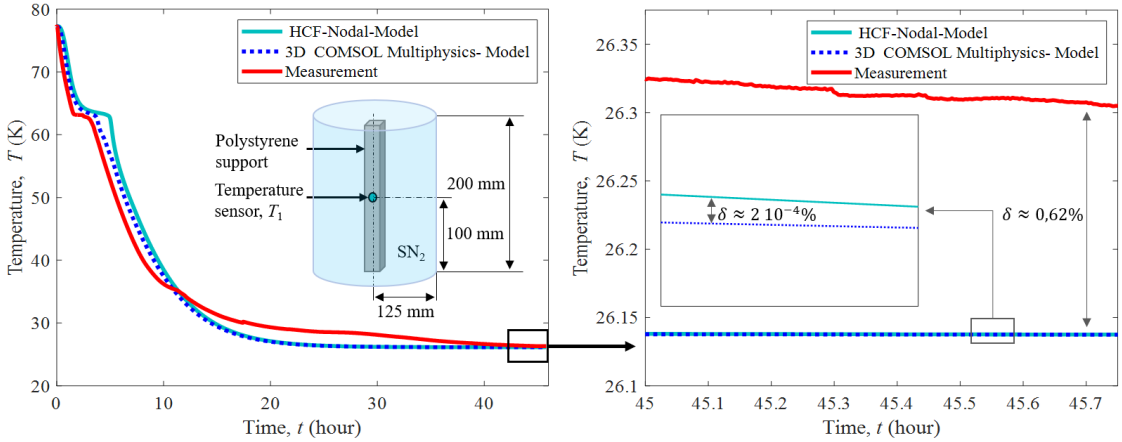

Figure 7. (a) Temperature at the center of the nitrogen bath as a function of time, (b) Steady state temperature in the range of 45 hours after the start of the cooling.

Model and FEM. In the HCF-Nodal-Model, an analytical specific heat function is defined that takes into account the liquid-solid transition at 63.1 K and the α-β phase transition. Several works were carried out in order to determine the various crystalline structures of solid nitrogen. Indeed, the work of T.A. Scott summarizes the experimental and theoretical literature on liquid and solid nitrogen where the different crystal structures and thermodynamic properties have been presented [16]. In this article, we are particularly interested in the liquid-solid phase change. For the α-β phase change temperature we rely on the work that is accepted as the best of Giauque and Clayton, i.e. $T_{\alpha\beta}$ =35.61 K [23].

In order to reduce the cooling time, the diameter of the bath was reduced to 600 mm. For this purpose, the space between the actual bath diameter and the copper exchanger was filled with polystyrene. The two models were compared, HCF-Nodal-Model and FEM, for 10 L of nitrogen in a bath of 250 mm diameter and 200 mm height.

Figure 7a shows the evolution of the temperature function of time for HCF-Nodal-Model, FEM and the experimental data. The temperature sensor T_1 is placed in the middle of the bath, i.e. at 100 mm from the bottom of the nitrogen bath and at a distance of 125 mm from the inner radius of the copper exchanger. We can see at first that both models have a good match with the measurement as they are both accurately predicting the cooling time needed to reach the steady state. Figure 7b shows that the

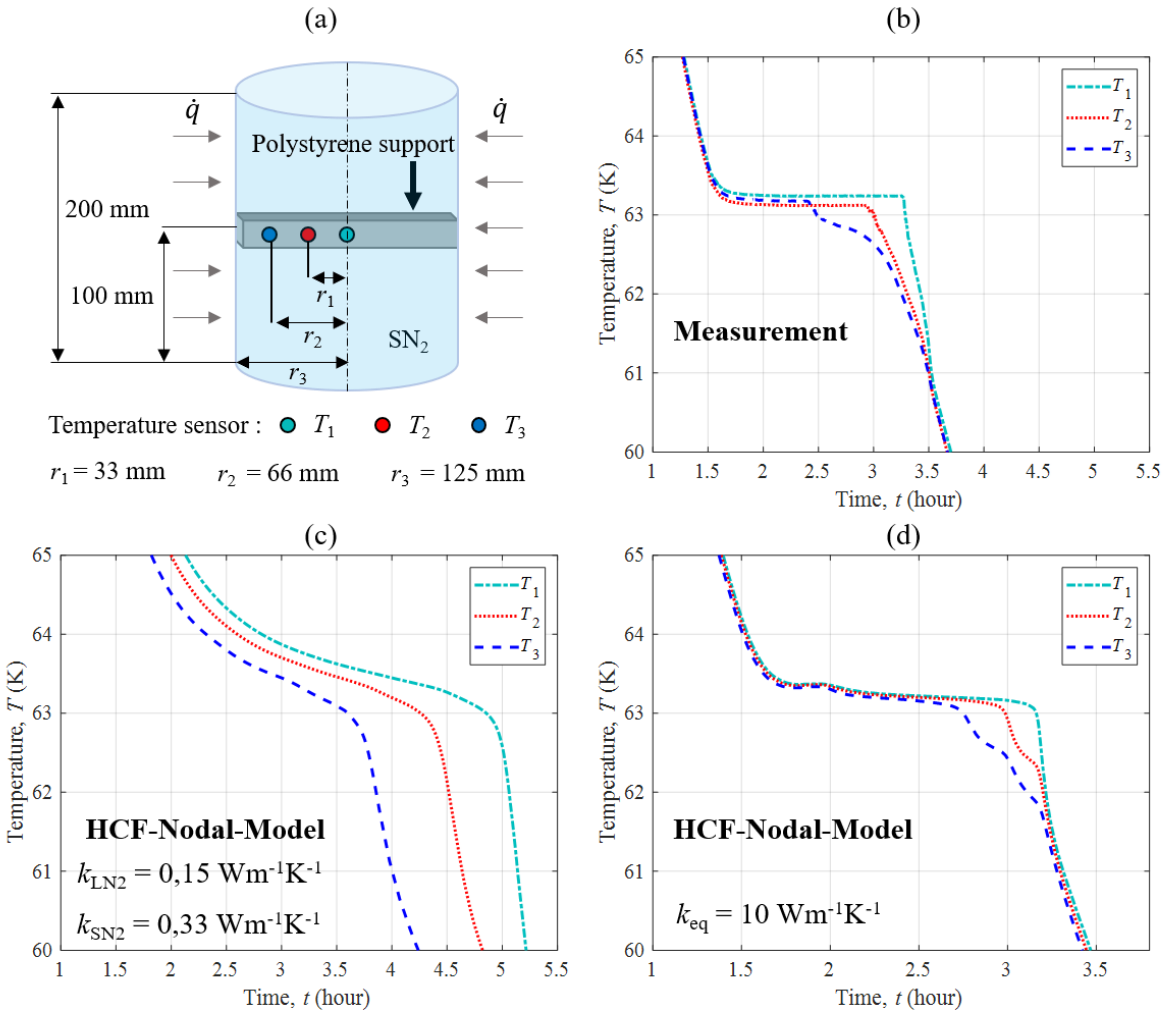

Figure 8. (a) Simplified diagram of the location of the temperature sensors in the nitrogen bath, (b), (c) and (d) sensor temperatures as a function of time of liquid-solid phase change for 10 L of liquid nitrogen.

relative error δ in steady state between HCF-Nodal-Model and FEM is negligible. The relative error between both models and measurements is almost negligible, about 0.62% in steady state. However, when the transition from liquid to solid phase occurs at 63.1 K, we can observe a difference between the models. We can explain this mismatch by two main reasons. Firstly, the HCF model does not consider the variation of the copper and nitrogen thermal conductivity with the temperature whereas FEM does. Secondly, in the LN_2 bath, HCF-Nodal-Model consider only the radial variation of the temperature while COMSOL consider the heat flux in every direction. Moreover, the simulation time of HCF is about 42.42 seconds for 32 nodes, which is 16.5 times faster than FEM for a simulation with 363 067 mesh nodes and 63 102 degrees of freedom. Thus, HCF-Nodal-Model appears to be a good compromise between computational cost and precision.

Additionally, there is a visible difference between the two models and the experiment that can be explained by the assumptions we made on the liquid bath. Indeed, both models are assuming a purely conductive heat transfer in the LN_2 and are completely neglecting the convection leading to an important underestimation of the effective thermal conductivity of the bath. This effective thermal conductivity considering conduction and convection is nonetheless difficult to determine a priori. Therefore, three sensors were placed in the radial direction of the bath to measure the temperature at different locations. As shown in figure 8a, T_1 sensor is located at the center of the bath, and T_2 and T_3 sensors are spaced 33 mm and 66 mm respectively from T_1. Figure 8b shows the temperature of these three sensors during the experiment at the liquid-solid phase change. The three temperatures are almost identical in the liquid state of the nitrogen and differ only during the transition. As was expected, the nitrogen located close to T_3 sensor is completely frozen at 2.38 h whereas this phase change is completed at 2.85 h and 3.52 h for T_2 and T_1 respectively. Figure 8c shows the temperature at the sensor locations for HCF-Nodal-Model with k_{LN2} = 0.15 W/m/K which is the conductivity value assumed beforehand considering only the conduction. A difference between the three sensors is visible in the liquid state whereas there is no visible gradient in the measurements. Therefore, figure 8d shows the HCF-Nodal-Model temperatures at the probe locations with an equivalent conductivity k_{LN2} = 10 W/m/K aiming to account for the convection a posteriori. For this new value, it appears that the modelling of the phase change is significantly more accurate than the initial assumption.

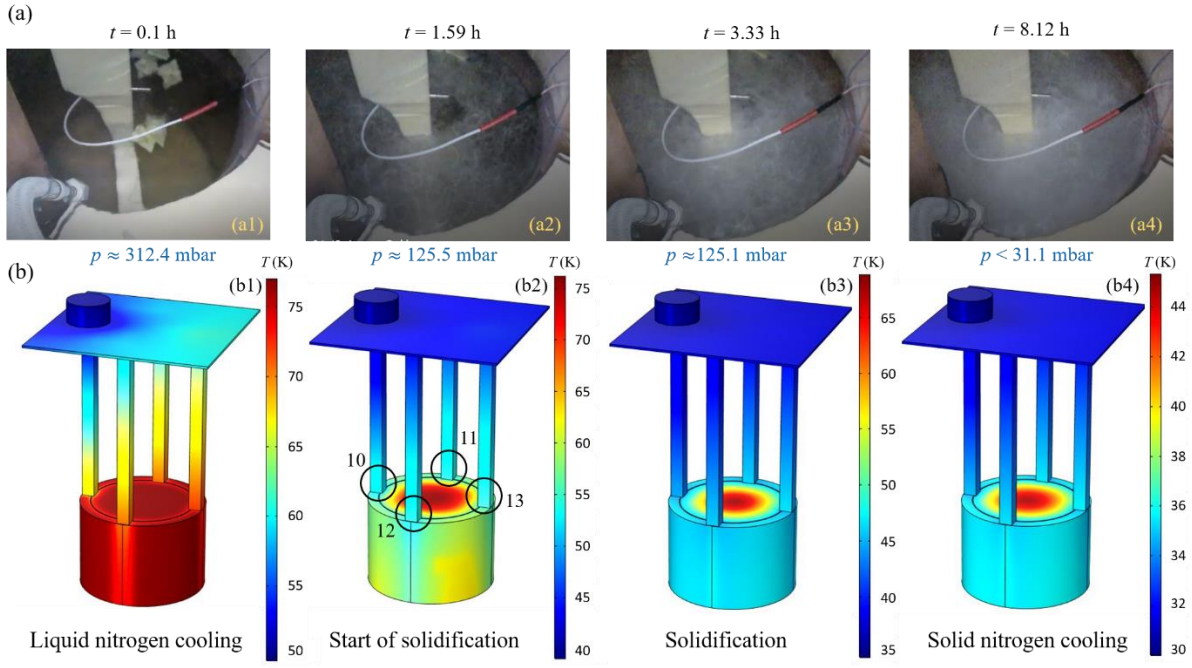

Figure 9. (a) Real images taken by a camera inside the cryostat at different times. (b) 3D view of the temperature profile of the cooling system and the nitrogen simulated by COMSOL Multiphysics.

Figures 9a and 9b show actual images taken by a camera inside the cryostat and the temperature profile of the cooling system and the nitrogen at different times. At the beginning of the phase change, at t =1.59 h, the temperatures of the four copper rods numbered 10, 11, 12 and 13 are very close, i.e. a temperature difference of about 2 K is observed. This condition guarantees a homogeneous cooling in the azimuthal and longitudinal direction of the nitrogen bath. Moreover, during the phase change the pressure inside the cryostat is almost constant and equal to about 125 mbar.

6. Conclusion

In this paper, a fast-analytical model is set up, based on the coupling of the nodal method to the heat capacity formulation in order to take into account the phase change of the fluid from liquid to solid state. This work was completed by a 3D simulation on COMSOL Multiphysics. The two models were compared by experimental work. In addition, the possibility of using an equivalent conductivity in the nitrogen bath to a posteriori account for convection was mentioned. On the practical side, the design of a cooling system to freeze the liquid nitrogen was successfully realized. Additionally, the cooling system guarantees an almost homogeneous cooling of the nitrogen bath in the azimuthal and longitudinal direction. This work will be continued in our laboratory and magnetization tests and characterizations of HTS bulks in frozen nitrogen at temperatures between 30 K and 60 K are planned soon.

References

[1] Berger K, Leveque J, Netter D, Douine B and Rezzoug A 2007 Influence of Temperature and/or Field Dependences of the E-J Power Law on Trapped Magnetic Field in Bulk YBaCuO *IEEE Trans. Appl. Supercond.* **17** 3028–31

[2] Kim K L, Song J B, Choi J H, Kim S H, Koh D Y, Seong K C, Chang H M and Lee H G 2010 The design and testing of a cooling system using mixed solid cryogen for a portable superconducting magnetic energy storage system *Supercond. Sci. Technol.* **23** 125006

[3] Yao W, Bascunan J, Kim W-S, Hahn S, Lee H and Iwasa Y 2008 A Solid Nitrogen Cooled MgB2 "Demonstration" Coil for MRI Applications *IEEE Trans. Appl. Supercond.* **18** 912–5

[4] Dorget R, Nouailhetas Q, Colle A, Berger K, Sudo K, Ayat S, Lévêque J, Koblischka M R, Sakai N, Oka T and Douine B 2021 Review on the Use of Superconducting Bulks for Magnetic Screening in Electrical Machines for Aircraft Applications *Materials* **14** 2847

[5] Hajiri G, Berger K, Dorget R, Lévêque J and Caron H 2021 Thermal and Electromagnetic Design of DC HTS Cables for the Future French Railway Network *IEEE Trans. Appl. Supercond.* **31** 1–8

[6] Colle A, Lubin T, Ayat S, Gosselin O and Leveque J 2020 Test of a Flux Modulation Superconducting Machine for Aircraft *J. Phys. Conf. Ser.* **1590** 012052

[7] Song J B, Kim K L, Kim K J, Lee J H, Kim H M, Kim W S, Yim S W, Kim H-R, Hyun O B and Lee H G 2008 The design, fabrication and testing of a cooling system using solid nitrogen for a resistive high- T_c superconducting fault current limiter *Supercond. Sci. Technol.* **21** 115023

[8] Fikiin K A 1996 Generalized numerical modelling of unsteady heat transfer during cooling and freezing using an improved enthalpy method and quasi-one-dimensional formulation *Int. J. Refrig.* **19** 132–40

[9] Le T D, Kim J H, Lee S J, Lee G-M, Sangjin K, Kim H-C and Kim H M 2015 Thermal analysis of a cooling system for a high-temperature superconducting magnet system *Inf. Jpn.* **18** 3133–9

[10] Makhtoumi M 2018 Numerical Solutions of Heat Diffusion Equation Over One Dimensional Rod Region *ArXiv180709588 Phys.*

[11] Rostami N, Feyzi M R, Pyrhonen J, Parviainen A and Niemela M 2013 Lumped-Parameter Thermal Model for Axial Flux Permanent Magnet Machines *IEEE Trans. Magn.* **49** 1178–84

[12] Goupil C, Ouerdane H, Zabrocki K, Seifert W, Hinsche N F and Müller E 2016 Thermodynamics and Thermoelectricity *Continuum Theory andModeling of Thermoelectric Elements* (John Wiley & Sons, Ltd) pp 1–74

[13] De Sousa W T B, Polasek A, Dias R, Matt C F T and de Andrade R 2014 Thermal–electrical analogy for simulations of superconducting fault current limiters *Cryogenics* **62** 97–109
[14] Lemmon E W and Jacobsen R T 2004 Viscosity and Thermal Conductivity Equations for Nitrogen, Oxygen, Argon, and Air *Int. J. Thermophys.* **25** 21–69
[15] Hanley H J M and Ely J F The Viscosity and Thermal Conductivity Coefficients of Dilute Nitrogen and Oxygen 22
[16] Scott T A 1976 Solid and liquid nitrogen *Phys. Rep.* **27** 89–157
[17] Cook T and Davey G 1976 The density and thermal conductivity of solid nitrogen and carbon dioxide *Cryogenics* **16** 363–9
[18] Stachowiak P, Sumarokov V V, Mucha J and Jeżowski A 1994 Thermal conductivity of solid nitrogen *Phys. Rev. B* **50** 543–6
[19] Suttell N, Zhang Z, Kweon J, Nes T, Kim C H, Pamidi S and Ordonez J C 2017 Investigation of solid nitrogen for cryogenic thermal storage in superconducting cable terminations for enhanced resiliency *IOP Conf. Ser. Mater. Sci. Eng.* **278** 012019
[20] The CH-110 single-stage Gifford-McMahon Cryocooler is SHI's highest-capacity 77K Cryocooler, with a first-stage capacity of 80/95 W @ 40 K (50/60 Hz). *SHI Cryog. Group*
[21] Cryogenic Technology Resources Cryogenics Material Properties *https://www.nist.gov/*
[22] Bagatskii M I, Kucheryavy V A, Manzhelii V G and Popov V A 1968 Thermal Capacity of Solid Nitrogen *Phys. Status Solidi B* **26** 453–60
[23] Giauque W F and Clayton J O 1933 The Heat Capacity and Entropy of Nitrogen. Heat of Vaporization. Vapor Pressures of Solid and Liquid. The Reaction 1/2 N2 + 1/2 O2 = NO from Spectroscopic Data *J. Am. Chem. Soc.* **55** 4875–89